A Theoretical Study of the H-Abstraction Reactions from HOI by Moist Air Radiolytic Products (H, OH, and O (3P)) and Iodine Atoms (2P3/2)

ARTICLE *in* THE JOURNAL OF PHYSICAL CHEMISTRY A · MAY 2011

Impact Factor: 2.69 · DOI: 10.1021/jp202760u

4 AUTHORS:

Hammaecher Catherine
Université des Sciences et Technologies de L…
11 PUBLICATIONS **33** CITATIONS
SEE PROFILE

Sebastien Canneaux
Université des Sciences et Technologies de L…
31 PUBLICATIONS **248** CITATIONS
SEE PROFILE

Florent Louis
Université des Sciences et Technologies de L…
45 PUBLICATIONS **397** CITATIONS
SEE PROFILE

Laurent Cantrel
Institut de Radioprotection et de Sûreté Nuc…
45 PUBLICATIONS **307** CITATIONS
SEE PROFILE

THE JOURNAL OF PHYSICAL CHEMISTRY A

ARTICLE

pubs.acs.org/JPCA

A Theoretical Study of the H-Abstraction Reactions from HOI by Moist Air Radiolytic Products (H, OH, and O (^{3}P)) and Iodine Atoms ($^2P_{3/2}$)

Catherine Hammaecher,[†] Sébastien Canneaux,[*,‡,∥] Florent Louis,[‡,∥] and Laurent Cantrel[§,∥]

[†]Université Catholique de Louvain, Bâtiment Lavoisier, Place L. Pasteur 1, B-1348 Louvain-la-Neuve, Belgium

[‡]PhysicoChimie des Processus de Combustion et de l'Atmosphère (PC2A) UMR 8522 CNRS/Lille1, Université Lille 1 Sciences et Technologies, Cité scientifique, Bât C11/C5, 59655 Villeneuve d'Ascq Cedex, France

[§]Institut de Radioprotection et de Sûreté Nucléaire, DPAM, SEMIC, Centre de Cadarache, BP3, 13115 Saint Paul Lez Durance, Cedex, France

[∥]Laboratoire de Recherche Commun IRSN-CNRS-Lille1 "Cinétique Chimique, Combustion, Réactivité" (C^{3}R), Centre de Cadarache, BP3, 13115 Saint Paul Lez Durance, Cedex, France

Supporting Information

ABSTRACT: The rate constants of the reactions of HOI molecules with H, OH, O (^{3}P), and I ($^2P_{3/2}$) atoms have been estimated over the temperature range 300−2500 K using four different levels of theory. Geometry optimizations and vibrational frequency calculations are performed using MP2 methods combined with two basis sets (cc-pVTZ and 6-311G(d,p)). Single-point energy calculations are performed with the highly correlated ab initio coupled cluster method in the space of single, double, and triple (pertubatively) electron excitations CCSD(T) using the cc-pVTZ, cc-pVQZ, 6-311+G(3df,2p), and 6-311++G(3df,3pd) basis sets. Reaction enthalpies at 0 K were calculated at the CCSD(T)/cc-pVnZ//MP2/cc-pVTZ (n = T and Q), CCSD(T)/6-311+G(3df,2p)//MP2/6-311G(d,p), and CCSD(T)/6-311++G(3df,3pd)//MP2/6-311G(d,p) levels of theory and compared to the experimental values taken from the literature. Canonical transition-state theory with an Eckart tunneling correction is used to predict the rate constants as a function of temperature. The computational procedure has been used to predict rate constants for H-abstraction elementary reactions because there are actually no literature data to which the calculated rate constants can be directly compared. The final objective is to implement kinetics of gaseous reactions in the ASTEC (accident source term evaluation code) program to improve speciation of fission products, which can be transported along the reactor coolant system (RCS) of a pressurized water reactor (PWR) in the case of a severe accident.

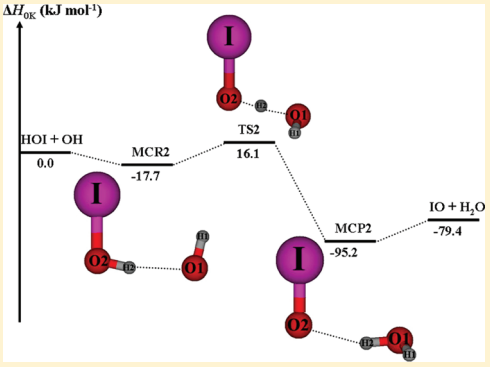

I. INTRODUCTION

In the case of a severe accident occurring to a nuclear pressurized water reactors (PWRs), the potential iodine release outside is a main safety issue because ^{131}I is a high radio-contaminant at short-term after the accident. The iodine fission product is emitted from the uranium damaged fuel, transported through the reactor coolant system (RCS) and next reaches, via the break, the nuclear containment building. From a safety point of view, iodine is extensively studied due to its high ability to form volatile compounds[1,2] which can be released and transported outside in the case of containment building leakages.

The french Institut de Radioprotection et de Sûreté Nucléaire (IRSN)[3] has undertaken a large program combining experimental and theoretical efforts in order to reduce the rather large uncertainties of the iodine concentration predictions in the containment building of a nuclear power plant. One open issue is to better model the transport of iodine through the RCS, which can have a great impact on iodine release.[4] The CHemistry of Iodine in the Primary circuit (CHIP)[5] is an international research program conducted by IRSN in the setting of the International Source Term Program (ISTP).[6] The main objectives are to determine the gaseous iodine quantity reaching the containment building and also to determine the thermokinetic experimental data for the main gaseous reactions governing the iodine behavior in the RCS. Therefore, these parameters could be used to develop and validate a physical chemistry model, which can be implemented in the ASTEC (accident source term evaluation code) severe accident simulation program.[7,8] Besides this experimental part, a theoretical approach using quantum chemistry tools has been carried out to accurately estimate the thermokinetic parameters for the main reactions involving iodine-containing species.[9,10] A first kinetic study[10] dealt with the kinetics of four reactions supposed to play a

Received: March 24, 2011
Revised: May 10, 2011
Published: May 27, 2011

key role on iodine speciation:

$$I\,(^2P_{3/2}) + H_2 = HI + H$$

$$I\,(^2P_{3/2}) + H_2O = HI + OH$$

$$I\,(^2P_{3/2}) + HI = H + I_2$$

$$I\,(^2P_{3/2}) + OH = HI + O\,(^3P)$$

It was the first step of a work consisting in the building of a detailed kinetic model, which will incorporate iodine-containing species. The work presented here is a second step and focuses on another set of iodine reactions, those involving the hydrogen abstraction from hypoiodous acid by H, OH, O (^{3}P), and I ($^2P_{3/2}$).

$$HOI + H \rightarrow IO + H_2 \qquad (R_1)$$

$$IO + H_2 \rightarrow HOI + H \qquad (R_{-1})$$

$$HOI + OH \rightarrow IO + H_2O \qquad (R_2)$$

$$IO + H_2O \rightarrow HOI + OH \qquad (R_{-2})$$

$$HOI + O\,(^3P) \rightarrow IO + OH \qquad (R_3)$$

$$IO + OH \rightarrow HOI + O\,(^3P) \qquad (R_{-3})$$

$$HOI + I\,(^2P_{3/2}) \rightarrow IO + HI \qquad (R_4)$$

$$IO + HI \rightarrow HOI + I\,(^2P_{3/2}) \qquad (R_{-4})$$

The H, OH, and O (^{3}P) species result from radiolysis of hydrogen and steam. The iodine atom is supposed to be the iodine species released from the degraded fuel because it is the most thermodynamic stable iodine species at high temperature. At high temperature, above 500 K, hypoiodous acid is under gaseous form.[11,12] HOI molecule is the most stable isomer form[13] of hypoiodous acid and it is a well-known reactive intermediate in iodine chemistry as it corresponds to the (+I) oxidation state.

Analyses of iodine releases coming from the two most famous nuclear severe accidents, Three Mile Island (1979) and Tchernobyl (1986) have showed that a significant fraction of total iodine release in the environment was under HOI gaseous form, respectively 18% in Three Mile Island[14] and 6% in Tchernobyl,[15] the other forms being particulates, molecular iodine and organic iodides. To obtain so high HOI fraction in gas-phase, one assumption is that HOI would be directly formed in the RCS and would have arrived in the containment building where a fraction could persist in the atmosphere. Iodine transport models consider the gaseous species at thermodynamic equilibrium, whatever the thermal conditions. These models do not allow the formation of HOI molecules at the break. The PHEBUS-FP[16] experimental results tend to show that this equilibrium assumption is not always valid, and some kinetic limitations can govern iodine speciation at the break,[17] thus kinetic constants have to be implemented in severe accident simulation software devoted to transport of iodine in the RCS.

Quantum chemistry calculations and TST kinetic models are used to compute the temperature dependence of the rate constants for the considered reactions in the temperature range (300−2500 K). To our knowledge, there is no kinetic data in the literature for the studied reactions but many computational works were carried out on the HOI molecule thermochemistry.[18−20] In this work, highly correlated ab initio quantum chemistry calculations are performed in order to directly compute the reaction barriers for the title reactions without any further adjustments of the energy. Among a wide variety of methods as described in our previous paper,[10] four levels of theory (CCSD(T)/cc-pVTZ//MP2/cc-pVTZ, CCSD(T)/cc-pVQZ//MP2/cc-pVTZ, CCSD(T)/6-311+G(3df,2p)//MP2/6-311G(d,p), and CCSD(T)/6-311++G(3df,3pd)//MP2/6-311G(d,p)) have been chosen in order to compute the thermokinetic parameters for the iodine reactions. The same methodology will be therefore employed for the estimation of the thermokinetic parameters for the reactions of HOI. The energetics of these reactions was used together with TST calculations to compute rate constants in the temperature range 300−2500 K.

This article is organized as follows. Computational methods are reported in section II, while the results are presented and discussed in section III.

II. COMPUTATIONAL METHODS

Ab initio calculations were performed using the Gaussian 03[21] software package. Reactants, transition states (TSs), molecular complexes, and products were fully optimized with the MP2[22] method using cc-pVTZ Dunning's correlation consistent basis set,[23] and the Pople-type 6-311G(d,p) basis set.[24] For the iodine atom, we used the cc-pVTZ-PP basis sets of Peterson et al.[25] which incorporate a relativistic pseudopotential (effective core potential) that largely accounts for scalar relativistic effects in iodine (these basis sets will be written without the PP term throughout the paper). We also employed an all-electron 6-311G basis[26] with valence basis sets augmented by the polarization d function.[27] All TSs have been characterized by one imaginary frequency (first-order saddle points) on the potential energy surface (PES). Special care was taken to determine minimum energy pathways (MEPs), performing intrinsic reaction coordinate analyses (IRC)[28] at all levels of theory, in order to confirm that a specific TS connects the different local minima. Vibrational frequencies and zero-point vibrational energies (ZPE) were determined within the harmonic approximation, at the same level of theory as that for geometries. The ab initio vibrational frequencies were multiplied by an appropriate scaling factor, which was obtained at each level of theory by plotting observed fundamentals for H_2, OH, HI, I_2, and H_2O versus calculated frequencies (0.961 and 0.955 for the MP2/cc-pVTZ and MP2/6-311G(d,p) levels of theory, respectively). For all stationary points (reactants, TS, molecular complexes, and products), single-point energy calculations were carried out at different high levels of theory using, in each case, the optimized MP2 geometrical parameters. Electronic energies were obtained employing the single and double coupled cluster theory with inclusion of a perturbative estimation for triple excitation (CCSD(T))[29] using (*i*) the cc-pVTZ and cc-pVQZ basis sets on geometries previously optimized with the Dunning-type cc-pVTZ basis sets, and (*ii*) the 6-311+G(3df,2p) and 6-311++G(3df,3pd) basis sets[24,27] on geometries obtained with the Pople-type 6-311G(d,p) basis set. The frozen-core approximation has been applied in CCSD(T) calculations, which implies that the inner-shells are excluded at estimating the correlation energy.

Spin−orbit coupling is of crucial importance, especially in the case of halogen atoms.[30,31] The potential energy of the iodine atom I ($^2P_{3/2}$) was obtained by subtracting one-third of the $^2P_{3/2}-^2P_{1/2}$ experimental splitting of the iodine atom[32] (30.29 kJ mol^{-1}) to the calculated potential energy of the iodine atom I (^2P). The minor spin−orbit corrections to the potential energies of HOI, IO, OH, O (^3P), and HI are −1.69,[33] −12.51,[34] −0.83,[35] −0.93,[32] and −2.09[36] kJ mol^{-1}, respectively. The potential energies of the molecular complexes either on the reactant (MCR) or on the product side (MCP) incorporate the spin−orbit corrections corresponding to those of the reactants or products. The values are −1.69, −2.52, −2.62, and −31.98 kJ mol^{-1} for MCR1, MCR2, MCR3, and MCR4, respectively. On the product side, the corresponding values are −12.51, −12.51, −13.34, and −14.60 kJ mol^{-1} for MCP1, MCP2, MCP3, and MCP4, respectively. In the TSs, the spin−orbit interaction is assumed to be negligibly small due to the spin delocalization. Similar results have been obtained for TS structures in the reaction of O (^3P) with C_2H_5I.[33]

The rate coefficient k for the four reactions under study involve a hydrogen-bonded adduct. It was initially analyzed according to the scheme advocated by Singleton and Cvetanovic[37] for prereactive complexes. We assume here that the reactions occur according to the mechanism involving a fast pre-equilibrium between the reactants and the prereactive complex (first step) followed by an abstraction leading to the postreactive complex and the products (second step). If k_1 and k_{-1} are the rate constants for the first step and k_2 corresponds to the second step, a steady-state analysis leads to a rate constant for the overall reaction, which can be written as

$$k = \frac{k_1 k_2}{k_{-1}} = \left(\frac{A_1 A_2}{A_{-1}}\right) \exp\left(-(E_1 + E_2 - E_{-1})/RT\right) \quad \text{(II-1)}$$

Since E_1 is zero, the net vibrationally adiabatic barrier E_0 for the overall reaction is given by the following relation:

$$E_0 = E_2 - E_{-1} = (E_{TS} - E_{MCR}) - (E_R - E_{MCR})$$
$$+ (ZPE_{TS} - ZPE_{MCR}) - (ZPE_R - ZPE_{MCR})$$
$$E_0 = E_{TS} - E_R + (ZPE_{TS} - ZPEE_R) \quad \text{(II-2)}$$

where E_R, E_{MCR}, and E_{TS} are the potential energies of the reactants, the prereactive complex, and the TS, respectively, whereas ZPE_R, ZPE_{MCR}, and ZPE_{TS} are their corresponding zero-point energy corrections. Thus, the vibrationally adiabatic barrier at high pressures can be calculated as the difference between the energy of the TS and the energy of the reactants, without having to obtain the prereactive complex. Applying basic statistical thermodynamic principles, the equilibrium constant $K_{R\text{-}MCR}$ of the fast pre-equilibrium between the reactants and the prereactive complex may be obtained as

$$K_{R\text{-}MCR} = \frac{Q_{MCR}}{Q_R} \exp[((E_R + ZPE_R) - (E_{MCR} + ZPE_{MCR}))/RT] \quad \text{(II-3)}$$

where Q_R, and Q_{MCR} are the total partition functions of the reactants and the prereactive complex, respectively. Under high pressure conditions, an equilibrium distribution of reactants is maintained in a unimolecular process, and the classical transition state theory (TST) formula can be applied[38] to calculate k_2:

$$k_2(T) = \Gamma(T) \times \frac{k_B T}{h} \times \frac{Q_{TS}(T)}{Q_{MCR}(T)}$$
$$\times \exp\left(\frac{(E_{MCR} + ZPE_{MCR}) - (E_{TS} + ZPE_{TS})}{k_B T}\right) \quad \text{(II-4)}$$

where $\Gamma(T)$ indicates the transmission coefficient used for the tunneling correction at temperature T, k_B is Boltzmann's constant, and h is Planck's constant.

The reaction path degeneracy is not included in this expression since the rotational symmetry numbers are already introduced in the calculation of the partition functions. The calculation of the reaction rate constants using the TST formulation given by eq II-4 requires the proper computation of partition functions of the prereactive complex and the TS. The total partition function $Q^X(T)$ of a species X can be cast in terms of the translational $Q^X_{trans}(T)$, electronic $Q^X_{elec}(T)$, rotational $Q^X_{rot}(T)$, and vibrational $Q_{vib}{}^X(T)$ partition functions:

$$Q^X(T) = Q^X_{trans}(T) Q^X_{elec}(T) Q^X_{rot}(T) Q^X_{vib}(T) \quad \text{(II-5)}$$

$\Gamma(T)$ is calculated as the ratio of the quantum mechanical to the classical barrier crossing rate, assuming an unsymmetrical one-dimensional Eckart function barrier.[39] This method approximates the potential by a one-dimensional function that is fitted to reproduce the zero-point energy corrected barrier, the enthalpy of reaction at 0 K, and the curvature of the potential curve at the TS. The numerical integration program of Brown[40] has been applied to obtain the $\Gamma(T)$ values at each level of theory. The existence of the complex in the entrance channel means that there are several rotational and vibrational energy levels from where tunneling may occur. We have assumed that a thermal equilibrium distribution of rovibrational energy levels is maintained, which corresponds to the high-pressure limiting behavior, and that all these levels, from the bottom of the well of the complex up to the top of the barrier, contribute to tunneling.

The rate constant calculations were performed over the temperature range of interest using the KISTHEP software suite.[41] The rate constants of the reactions of HOI molecules with OH (reaction R_2), O (^3P) (reaction R_3), and I (^2P) (reaction R_4) are calculated as described above. In the case of the reaction of HOI molecules with H (reaction R_1), although the prereactive complex structure has been located on the PES at all levels of theory, the relative enthalpies calculated at 0 K exhibit small differences by comparison to the reactants (less than −0.6 kJ mol^{-1}). In the case of the reaction R_1, canonical TST[38] is used to predict the temperature dependence of the rate constants. Accordingly, the rate constants $k(T)$ are computed using the following expression:

$$k(T) = \Gamma(T) \times \frac{k_B T}{h} \times \frac{Q_{TS1}(T)}{Q_{HOI}(T) Q_H(T)}$$
$$\times \exp\left(-\frac{E_0}{k_B T}\right) \quad \text{(II-6)}$$

where the terms $Q_{TS1}(T)$, $Q_{HOI}(T)$, and $Q_H(T)$ are the total partition functions for the TS1, the HOI molecule, and the hydrogen atom at the temperature T. In eq II-6, the vibrationally

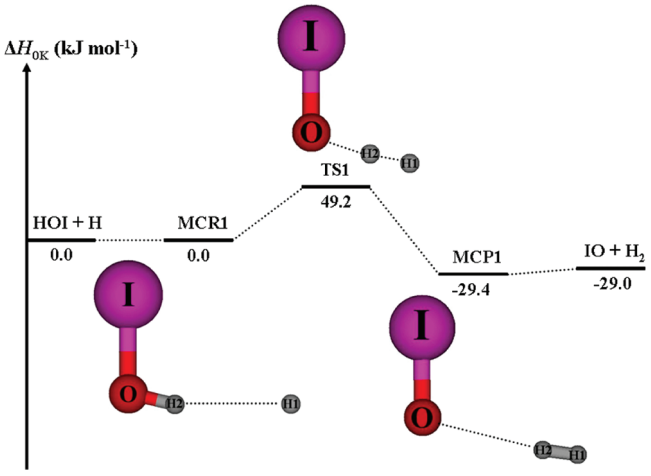

Figure 1. Potential energy profiles for the HOI + H reaction system calculated at the CCSD(T)/cc-pVTZ//MP2/cc-pVTZ level of theory.

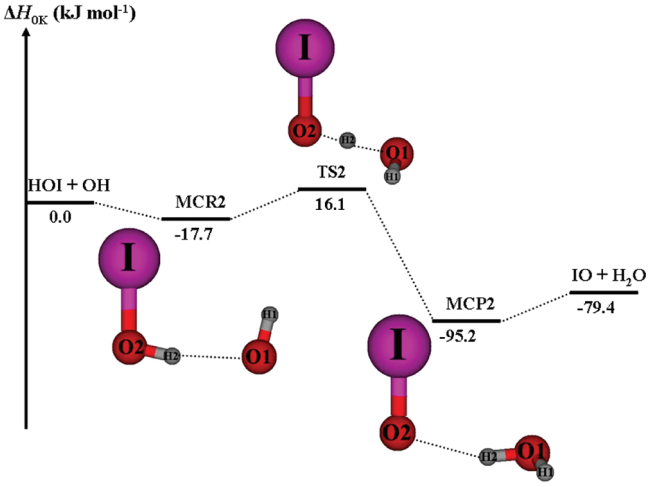

Figure 2. Potential energy profiles for the HOI + OH reaction system calculated at the CCSD(T)/cc-pVTZ//MP2/cc-pVTZ level of theory.

adiabatic barrier height, E_0, is computed as the energy difference between the TS1 and the reactants HOI and H.

The rate constants of the reverse reactions are obtained using the following expression:

$$k_{\text{reverse}}(T) = k_{\text{forward}}(T) \times K_{\text{eq}}(T) \qquad \text{(II-7)}$$

where $K_{\text{eq}}(T)$ is the equilibrium constant between the reactants and the products. $K_{\text{eq}}(T)$ is calculated at the same level of theory as $k_{\text{forward}}(T)$.

III. RESULTS AND DISCUSSION

1. Geometric Parameters and Vibrational Frequencies. Figures 1−4 show the structures and atom numbering of the determined TSs and molecular complexes for the four studied reactions. Tables 1−4 list the structural parameters and unscaled imaginary vibrational frequencies calculated for the TSs and molecular complexes (MCR and MCP) at the MP2/cc-pVTZ and MP2/6-311G(d,p) levels of theory, respectively. More detailed information regarding optimized geometric parameters

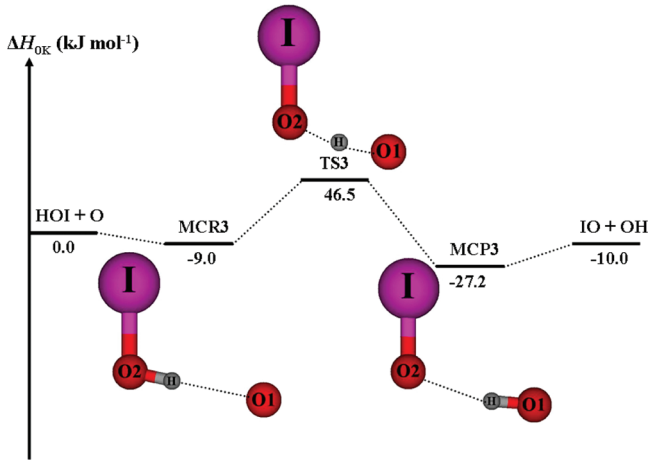

Figure 3. Potential energy profiles for the HOI + O (^{3}P) reaction system calculated at the CCSD(T)/cc-pVTZ//MP2/cc-pVTZ level of theory.

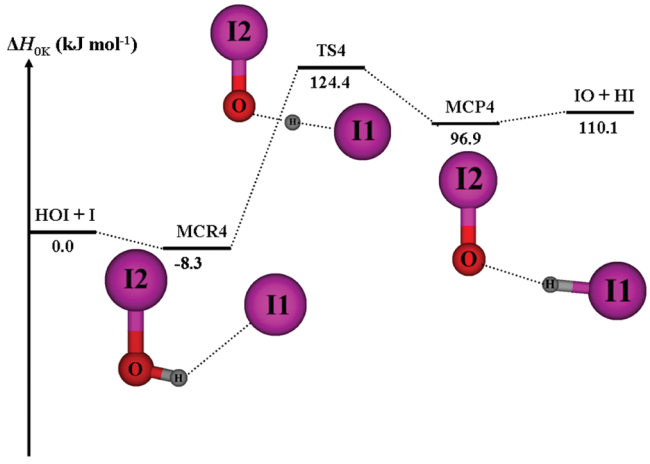

Figure 4. Potential energy profiles for the HOI + I ($^2P_{3/2}$) reaction system calculated at the CCSD(T)/cc-pVTZ//MP2/cc-pVTZ level of theory.

(reactants and products) and vibrational frequencies (reactants, TSs, molecular complexes and products) are given in Tables 1S-3S of the Supporting Information.

Geometric Parameters. Transition States. The TS structures of H-abstraction reactions of HOI by H, OH, O (^{3}P), and I ($^2P_{3/2}$) are not linear with bond angles values varying from about 145 to 170°. The unpaired electron on the open-shell species attacks the H−O σ-bond of the HOI molecule, and the two electrons of the σ-bond become unpaired. The main change in the geometrical structure of the TS can be characterized by the L parameter, defined as the ratio of the increase in the length of the bond being broken and the elongation of the bond being formed.[42] This parameter provides a reliable measure of the reactant- or product-like character of the concomitant TS. Large L values correspond to product-like TSs, while smaller values correspond to reactant-like TSs. The calculated values of the L parameter for each studied reaction are given in Tables 1−4. These values are all greater than 1 for the two levels of theory and reactions of HOI with H, O (^{3}P), and I ($^2P_{3/2}$) atoms. The TS structures are indeed product-like. In the case of the reaction of HOI with the

dx.doi.org/10.1021/jp202760u |J. Phys. Chem. A 2011, 115, 6664–6674

Table 1. Structural Parameters[a] and Unscaled Imaginary Frequencies for the TSs and Molecular Complexes of the Reaction (R_1) at Different Levels of Theory

HOI + H → IO + H_2 (R_1)			
parameter	species	MP2/cc-pVTZ	MP2/6-311G(d,p)
r(I−O), Å	MCR1	1.992 (1.991)	2.041
	TS1	1.934	1.973
	MCP1	1.886	1.937
r(O−H2), Å	MCR1	0.967 (0.967)	0.966
	TS1	1.282	1.273
	MCP1	2.619	2.638
r(H2−H1), Å	MCR1	3.090 (2.349)	3.116
	TS1	0.836	0.838
	MCP1	0.739	0.739
θ(IOH2), °	MCR1	103.1 (103.0)	102.5
	TS1	109.8	110.6
	MCP1	105.8	105.5
θ(OH2H1), °	MCR1	80.4 (167.0)	83.2
	TS1	174.0	171.3
	MCP1	172.2	174.9
ϕ(IOH2H1), °	MCR1	−102.0 (7.6)	−106.5
	TS1	0.0	0.0
	MCP1	0.0	0.0
L[b]		3.2	3.1
$\nu\ddagger$, cm^{-1}		2149i	2112i

[a] Values in parentheses correspond to the structural parameters for MCR1 in which H1 is in the plane of IOH2. [b] The parameter L is defined as the ratio of the increase in the length of the bond being broken and the elongation of the bond being formed, each with respect to its equilibrium value in the reactant and the product.

Table 2. Structural Parameters and Unscaled Imaginary Frequencies for the TSs and Molecular Complexes of the Reaction (R_2) at Different Levels of Theory

HOI + OH → IO + H_2O (R_2)			
parameter	species	MP2/cc-pVTZ	MP2/6-311G(d,p)
r(I−O2), Å	MCR2	1.984	2.033
	TS2	1.973	2.005
	MCP2	1.879	1.938
r(O2−H2), Å	MCR2	0.974	0.971
	TS2	1.094	1.096
	MCP2	2.041	2.093
r(H2−O1), Å	MCR2	1.956	1.979
	TS2	1.222	1.210
	MCP2	0.964	0.961
r(O1−H1), Å	MCR2	0.970	0.969
	TS2	0.967	0.965
	MCP2	0.959	0.958
θ(IO2H2), °	MCR2	102.3	102.0
	TS2	106.5	107.2
	MCP2	104.3	104.8
θ(O2H2O1), °	MCR2	168.4	170.0
	TS2	149.1	146.7
	MCP2	159.5	155.5
θ(H2O1H1), °	MCR2	104.5	111.2
	TS2	103.3	102.2
	MCP2	103.6	102.4
ϕ(IO2H2O1), °	MCR2	−1.0	3.3
	TS2	86.0	83.9
	MCP2	6.2	14.4
ϕ(O2H2O1), °	MCR2	0.7	−1.3
	TS2	29.9	39.2
	MCP2	110.7	95.5
L[a]		0.5	0.5
$\nu\ddagger$, cm^{-1}		3061i	3038i

[a] The parameter L is defined as the ratio of the increase in the length of the bond being broken and the elongation of the bond being formed, each with respect to its equilibrium value in the reactant and the product.

OH radical, a relatively "early" TS on the PES is found at both levels of theory where the breaking bond O2−H2 is stretched by only a small amount from its equilibrium valued in HOI (≈ 0.96 Å). This is reflected by the values of the L parameter, which are lower than 1. All these results are in agreement with Hammond's postulate,[43] which predicts a product-like character for the TS when the reaction is endoergic and a reactant-like character with an exoergic reaction. There is little influence of the basis set (cc-pVTZ and 6-311G(d,p)) on the calculated values of the L parameter with the exception of the reaction of HOI with I ($^2P_{3/2}$) atoms R_4.

Molecular Complexes. The IRC calculations at each level of theory have revealed that the MEPs connect the TSs to loosely bound dipole−dipole complexes in both the forward and backward directions.

Reaction R_1. TS1 is connected to the IOH···H reactant complex (MCR1) and also to the IO···HH product complex (MCP1). When going from the TS1 structure to the products, the reaction proceeds with a dihedral angle ϕ(IO2H2H1) equal to 0°. On the reactant side, the IRC calculations lead to a branching point on the PES which conducts to two different structures for MCR1. The most stable structure is found in which the H1 atom is out of the plane (ϕ(IO2H2H1) equal to −102.0 and −106.5° at the MP2/cc-pVTZ and MP2/6-311G(d,p) levels of theory, respectively). Another structure for MCR1 has been located only at the MP2/cc-pVTZ level of theory in which the H1 atom is nearly in the plane of IO2H (ϕ(IO2H2H1) = 7.6°).

The structures of MCR1 and MCP1 are similar to that of TS1, with the characteristic difference that the emerging new bond H2−H1 is much shorter in the TS than in the MCR1 complex (0.836 compared to 3.090 Å calculated at the MP2/cc-pVTZ level of theory, respectively), and the breaking bond O−H2 is much shorter in the TS than that in the MCP1 complex (1.282 compared to 2.619 Å calculated at the MP2/cc-pVTZ level of theory, respectively).

Reaction R_2. TS2 is connected to the IOH···OH reactant complex (MCR2) and also to the IO···HOH product complex (MCP2). When the oxygen atom from the hydroxyl radical approaches the HOI molecule, it forms an intermolecular bond H2−O1 of 1.956 Å at the MP2/cc-pVTZ level of theory. On the product side, the structure of MCP2 has been determined with an intermolecular bond O2−H2 of 2.041 Å.

Reaction R_3. TS3 is connected to the IOH···O reactant complex (MCR3) and also to the IO···HO product complex (MCP3). The O atom approaches the HOI molecule in a

Table 3. Structural Parameters and Unscaled Imaginary Frequencies for the TSs and Molecular Complexes of the Reaction (R_3) at Different Levels of Theory

HOI + O (^{3}P) → IO + OH (R_3)			
parameter	species	MP2/cc-pVTZ	MP2/6-311G(d,p)
r(I−O2), Å	MCR3	1.988	2.036
	TS3	1.917	1.964
	MCP3	1.878	1.938
r(O2−H), Å	MCR3	0.969	0.967
	TS3	1.183	1.196
	MCP3	2.003	2.032
r(H−O1), Å	MCR3	2.108	2.179
	TS3	1.119	1.105
	MCP3	0.973	0.970
θ(IO2H), °	MCR3	102.6	102.2
	TS3	113.4	113.9
	MCP3	109.0	115.6
θ(O2HO1), °	MCR3	178.8	172.5
	TS3	168.1	164.6
	MCP3	166.3	171.5
ϕ(IO2HO1), °	MCR3	−76.5	0.0
	TS3	0.0	0.0
	MCP3	−0.9	0.0
L^a		1.4	1.7
ν‡, cm^{-1}		2625i	2933i

[a] The parameter L is defined as the ratio of the increase in the length of the bond being broken and the elongation of the bond being formed, each with respect to its equilibrium value in the reactant and the product.

Table 4. Structural Parameters and Unscaled Imaginary Frequencies for the TSs and Molecular Complexes of the Reaction (R_4) at Different Levels of Theory

HOI + I ($^2P_{3/2}$) → IO + HI (R_4)			
parameter	species	MP2/cc-pVTZ	MP2/6-311G(d,p)
r(I2−O), Å	MCR4	1.989	2.037
	TS4	1.883	1.945
	MCP4	1.880	1.937
r(O−H), Å	MCR4	0.971	0.968
	TS4	1.431	1.403
	MCP4	2.052	2.166
r(H−I1), Å	MCR4	2.705	2.901
	TS4	1.678	1.700
	MCP4	1.609	1.613
θ(I2OH), °	MCR4	102.8	102.1
	TS4	116.8	118.8
	MCP4	107.6	112.7
θ(OHI1), °	MCR4	175.2	162.6
	TS4	166.1	164.4
	MCP4	167.9	172.5
ϕ(I2OHI1), °	MCR4	−10.3	0.0
	TS4	64.6	62.7
	MCP4	0.0	−0.2
L^a		4.6	5.8
ν‡, cm^{-1}		685i	1027i

[a] The parameter L is defined as the ratio of the increase in the length of the bond being broken and the elongation of the bond being formed, each with respect to its equilibrium value in the reactant and the product.

conformation where the dihedral angle ϕ(IO2HO1) is equal to −76.5° at the MP2/cc-pVTZ level of theory. Despite exhaustive searches at the MP2/cc-pVTZ level of theory on the PES, no stationary point was found for a conformation in which the O atom will be in the plane of the HOI molecule. When using the 6-311G(d,p) basis set, only one structure for MCR3 was located on PES with ϕ(IO2HO1) = 0°. The intermolecular bond length H−O1 in MCR3 was estimated to be about 2.108 Å at the MP2/cc-pVTZ level of theory. The MCP3 structure is characterized by an intermolecular bond length O2−H of 2.003 Å at the MP2/cc-pVTZ level of theory.

Reaction R_4. TS4 is connected to the IOH···I reactant complex (MCR4) and also to the IO···HI product complex (MCP4). When the iodine atom approaches the hypoiodous acid on the doublet PES, it forms an intermolecular bond H−I1 of 2.705 Å at the MP2/cc-pVTZ level of theory. On the product side, the structure of MCP4 has been determined with an intermolecular bond O−H of 2.052 Å at the MP2/cc-pVTZ level of theory.

Vibrational Frequencies. In all cases, the eigenvector in the TS corresponding to the imaginary frequency is primarily a motion of the atom being transferred. In the case of the reactions of HOI with O (^{3}P) and I ($^2P_{3/2}$), the values of the imaginary frequency are found to be larger with the 6-311G(d,p) basis set than the ones obtained with the cc-pVTZ basis set. These values are about 10 and 50% larger using the cc-pVTZ basis set.

2. Energetics. Table 5 lists for the four studied reactions the reaction enthalpies Δ_rH at 0 K calculated at the different levels of theory. The results obtained indicate that the reactions of HOI with H, OH, and O (^{3}P) are predicted to be exothermic while the reaction of HOI with I ($^2P_{3/2}$) is endothermic. These results show that the computed reaction enthalpies do not depend on the geometry optimization level of theory. The basis set in the CCSD(T) single-point energy calculation does significantly affect the Δ_rH at 0 K values. Increasing the basis sets size from cc-pVTZ to cc-pVQZ changes the values by about +0.8, −5.3, −7.0, and −6.8 kJ mol^{-1} for reactions R_1, R_2, R_3, and R_4, respectively. Less marked trends are observed when using the Pople-type basis sets. Increasing the basis sets size from 6 to 311+G(3df,2p) to 6-311++G(3df,3pd) changes the values by about +4.0, 1.5, 0.2, and −2.7 kJ mol^{-1} for reactions R_1, R_2, R_3, and R_4, respectively.

The Δ_rH at 0 K values have been calculated using the literature heats of formation $\Delta_fH°$ at 0 K for the species of interest (see Table 4S in the Supporting Information).[18,44,45] Their values as well as their associated uncertainties are also listed for each reaction in Table 5. The calculated Δ_rH at 0 K calculated at the CCSD(T)/cc-pVQZ//MP2/cc-pVTZ level of theory are −28.2, −84.7, −17.0, and 103.3 kJ mol^{-1} for reactions R_1, R_2, R_3, and R_4, respectively. The experimental literature values are (−37.3 ± 5.0), (−98.6 ± 6.3), (−29.7 ± 6.3), and (100.1 ± 5.3) kJ mol^{-1} for reactions R_1, R_2, R_3, and R_4, respectively. The calculated values are close to their literature counterparts, especially if the experimental uncertainties are taken into consideration. Similar trends were noticed in our previous work on the reactivity of iodine atoms between the computed Δ_rH at 0 K and the corresponding literature values.[10]

Table 5. Reaction Enthalpies $\Delta_r H$ Calculated at 0 K in kJ mol^{-1} at Different Levels of Theory Including Spin-Orbit Corrections

SPC level of theory	HOI + H → IO + H_2 (R_1)	HOI + OH → IO + H_2O (R_2)	HOI + O (^{3}P) → IO + OH (R_3)	HOI + I ($^2P_{3/2}$) → IO + HI (R_4)
CCSD(T)/cc-pVTZ//MP2/cc-pVTZ	−29.0	−79.4	−10.0	110.1
CCSD(T)/cc-pVQZ//MP2/cc-pVTZ	−28.2	−84.7	−17.0	103.3
CCSD(T)/6-311+G(3df,2p)//MP2/6-311G(d,p)	−30.1	−85.1	−17.4	109.8
CCSD(T)/6-311++G(3df,3pd)//MP2/6-311G(d,p)	−26.1	−83.6	−17.2	107.1
experimental value (literature)[18,44,45]	*-37.3 ± 5.0*	*-98.6 ± 6.3*	*-29.7 ± 6.3*	*100.1 ± 5.3*

Table 6. Vibrationally Adiabatic Barriers E_0 Calculated in kJ mol^{-1} at Different Levels of Theory Including Spin-Orbit Corrections

SPC level of theory	HOI + H → IO + H_2 (R_1)	HOI + OH → IO + H_2O (R_2)	HOI + O (^{3}P) → IO + OH (R_3)	HOI + I ($^2P_{3/2}$) → IO + HI (R_4)
CCSD(T)/cc-pVTZ//MP2/cc-pVTZ	49.2	16.1	46.5	124.4
CCSD(T)/cc-pVQZ//MP2/cc-pVTZ	49.6	15.9	42.0	115.5
CCSD(T)/6-311+G(3df,2p)//MP2/6-311G(d,p)	52.6	20.3	41.1	124.2
CCSD(T)/6-311++G(3df,3pd)//MP2/6-311G(d,p)	51.0	16.8	36.7	119.0

Table 7. Relative Enthalpies at 0 K in kJ mol^{-1} for the Prereactive and Postreactive Complexes at Different Levels of Theory including Spin-Orbit Corrections[a]

	HOI + H → IO + H_2 (R_1)			HOI + OH → IO + H_2O (R_2)	
SPC level of theory	MCR1		MCP1	MCR2	MCP2
CCSD(T)/cc-pVTZ//MP2/cc-pVTZ	0.0	0.2[b]	−29.4 (−0.5)	−17.7	−95.2 (−15.8)
CCSD(T)/cc-pVQZ//MP2/cc-pVTZ	0.1	−0.4[b]	−27.6 (0.6)	−16.5	−99.7 (−15.0)
CCSD(T)/6-311+G(3df,2p)//MP2/6-311G(d,p)	0.6		−28.1 (2.0)	−16.1	−98.3 (−13.3)
CCSD(T)/6-311++G(3df,3pd)//MP2/6-311G(d,p)	0.1		−25.0 (1.1)	−16.8	−97.7 (−14.1)

	HOI + O (^{3}P) → IO + OH (R_3)		HOI + I ($^2P_{3/2}$) → IO + HI (R_4)	
SPC level of theory	MCR3	MCP3	MCR4	MCP4
CCSD(T)/cc-pVTZ//MP2/cc-pVTZ	−9.0	−27.2 (−17.2)	−8.3	96.9 (−13.1)
CCSD(T)/cc-pVQZ//MP2/cc-pVTZ	−8.4	−33.3 (−16.3)	−10.9	89.6 (−13.7)
CCSD(T)/6-311+G(3df,2p)//MP2/6-311G(d,p)	−9.5	−33.2 (−15.7)	−11.3	97.5 (−12.3)
CCSD(T)/6-311++G(3df,3pd)//MP2/6-311G(d,p)	−10.6	−33.8 (−16.6)	−13.1	93.9 (−13.2)

[a] Values in parentheses correspond to the relative enthalpies at 0 K in kJ mol^{-1} with respect to the products. [b] MCR1 in which H1 is in the plane of IOH2.

Table 6 shows for reactions R_1, R_2, R_3, and R_4 the computed vibrationally adiabatic barriers at the different levels of theory. The H-abstraction from HOI by H, OH, and O (^{3}P) appears to have a relatively small electronic barrier by comparison to the one obtained in the reaction of HOI with I ($^2P_{3/2}$). The vibrationally adiabatic barriers are sensitive to the basis set employed in the CCSD(T) single-point energy calculation. Increasing the basis sets size either from cc-pVTZ to cc-pVQZ (for reactions R_3 and R_4) or from 6 to 311+G(3df,2p) to 6-311++G(3df,3pd) (for reactions R_1, R_2, R_3, and R_4) tends to decrease the E_0 values. If we compare the results obtained using the CCSD(T)/6-311+G(3df,2p) and CCSD(T)/cc-pVTZ levels of theory, it can be seen that the E_0 values are close to each other within about 5 kJ mol^{-1} and independent of the geometry level. The same trends are observed using the CCSD(T)/6-311++G-(3df,3pd) and CCSD(T)/cc-pVQZ levels of theory.

Table 7 lists the relative enthalpies at 0 K for the prereactive and postreactive complexes at different levels of theory. It can be seen that the prereactive (MCR1) and postreactive (MCP1) complexes are not more stable than the reactants HOI + H and IO + H_2, respectively (ΔH_{0K} < 2 kJ mol^{-1}). For all other prereactive complexes (MCR2, MCR3, and MCR4), the stabilization energies at 0 K are in the range of −8 to −18 kJ mol^{-1}. Increasing the basis set size has little effect on the relative enthalpies of the prereactive complexes (MCR1, MCR2, MCR3, and MCR4) and the postreactive complexes (MCP1, MCP2, MCP3, and MCP4).

3. Kinetic Parameters Calculations. *Rate Constants.* The calculations of the temperature dependence of rate constants over the temperature range 300−2500 K have been performed at different levels of theory for the reactions of HOI with H, OH, O (^{3}P), and I ($^2P_{3/2}$) using an asymmetrical Eckart potential for the tunneling

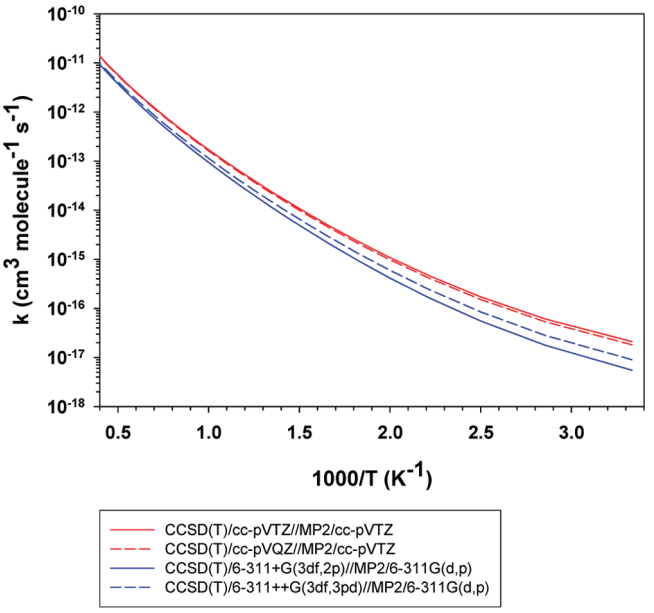

Figure 5. Temperature dependence of the rate constant of the reaction HOI + H → IO + H_2 (R_1).

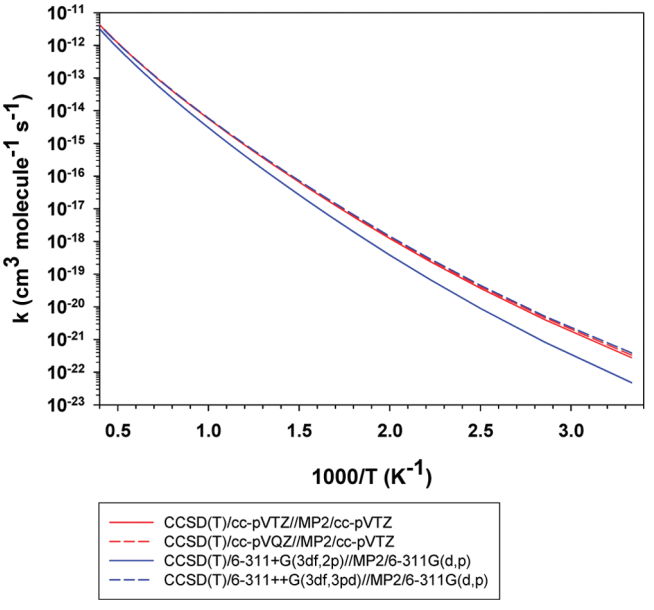

Figure 6. Temperature dependence of the rate constant of the reaction IO + H_2 → HOI + H (R_{-1}).

correction whose values are gathered in Tables 5S−8S of the Supporting Information. The results of the calculated rate constants for the eight studied elementary reactions at four levels of theory for six different temperatures (300, 600, 1000, 1500, 2000, and 2500 K) are shown in Tables 9S−16S of the Supporting Information. Figures 5−12 present the corresponding temperature dependence of the rate constants. As shown for example in Table 9S for the reaction R_1, the computed rate constants at 300 K range from 0.5 to 2.0 × 10^{-17} cm^3 $molecule^{-1}$ s^{-1}, showing the small dependence of the rate constant on the level of theory. It can be noticed that the values computed at the CCSD(T)/cc-pVQZ and CCSD(T)/cc-pVTZ levels of theory on MP2/cc-pVTZ optimized geometries

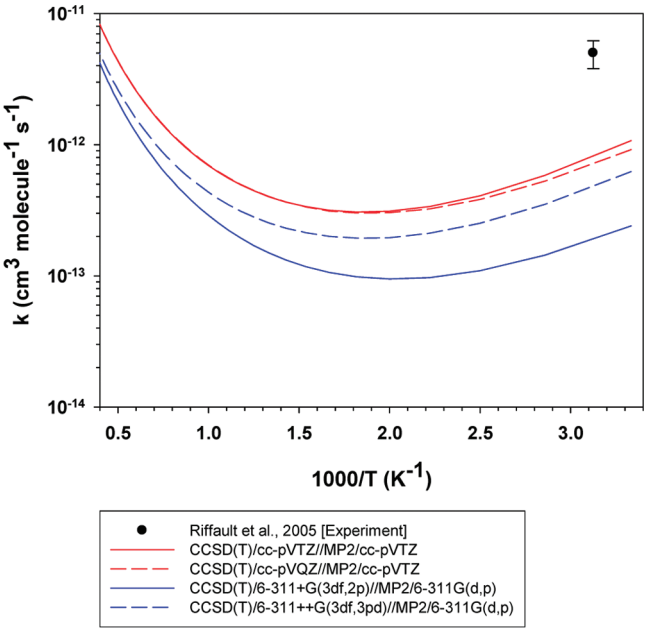

Figure 7. Temperature dependence of the rate constant of the reaction HOI + OH → IO + H_2O (R_2).

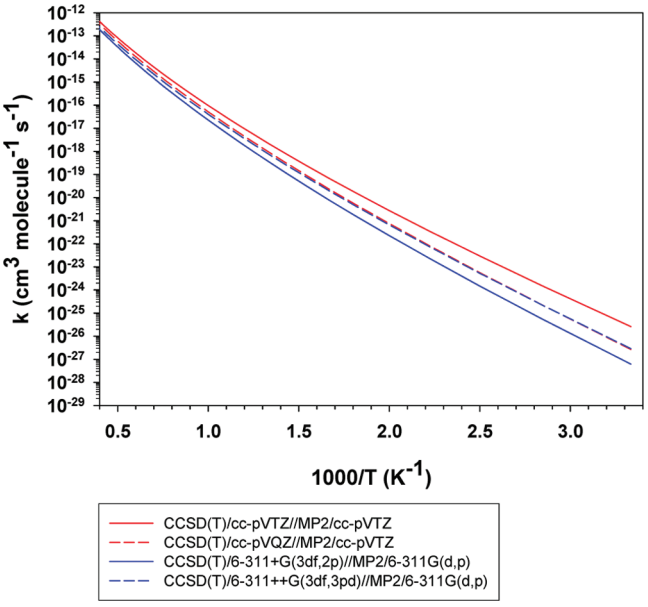

Figure 8. Temperature dependence of the rate constant of the reaction IO + H_2O → HOI + OH (R_{-2}).

are close to each other. The calculated rate constants using CCSD(T) energies with the 6-311+G(3df,2p) and 6-311++G(3df,3pd) basis sets differ only by a factor of about 2 at 300 K. Similar trends at 300 K can be noticed for the other reactions. The biggest difference in the calculated rate constants is observed in the case of the reaction R_4 between the CCSD(T)/cc-pVTZ and CCSD(T)/cc-pVQZ energies using MP2/cc-pVTZ optimized geometries. The influence of the basis set size on the calculated rate constants is, however, less and less marked as the temperature rises.

HOI + OH → IO + H_2O (R_2). The global reaction of HOI with OH has been studied by Riffault et al.[46] using the mass

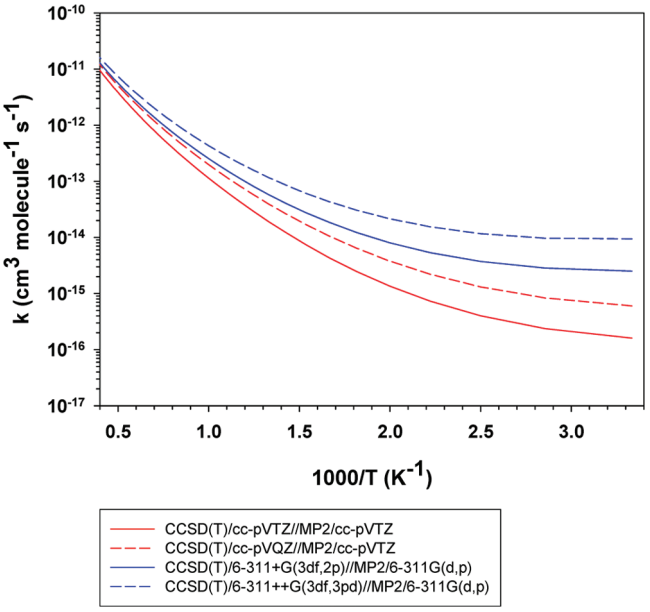

Figure 9. Temperature dependence of the rate constant of the reaction HOI + O (^{3}P) → IO + OH (R_3).

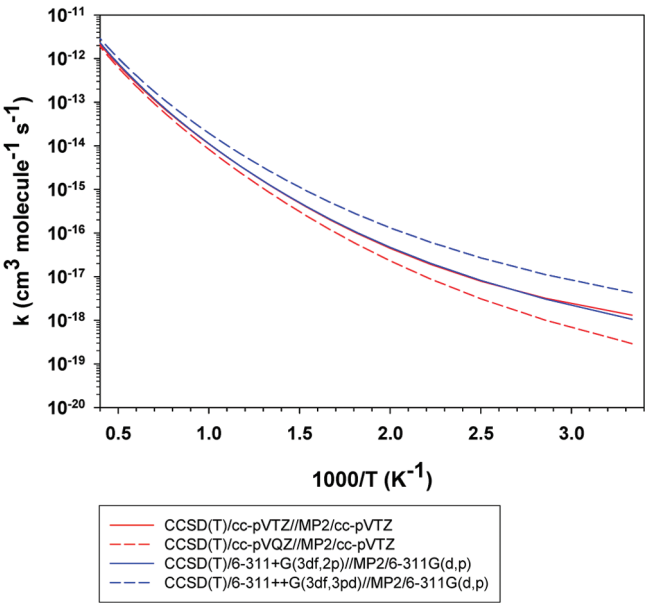

Figure 10. Temperature dependence of the rate constant of the reaction IO + OH → HOI + O (^{3}P) (R_{-3}).

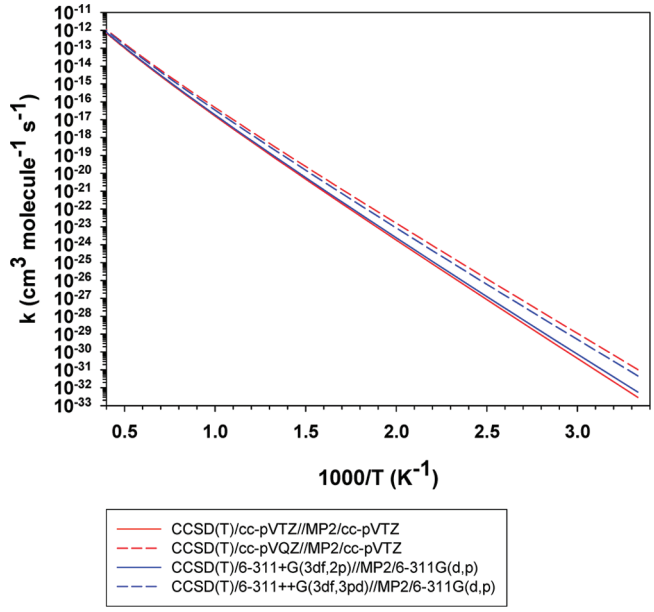

Figure 11. Temperature dependence of the rate constant of the reaction HOI + I ($^2P_{3/2}$) → IO + HI (R_4).

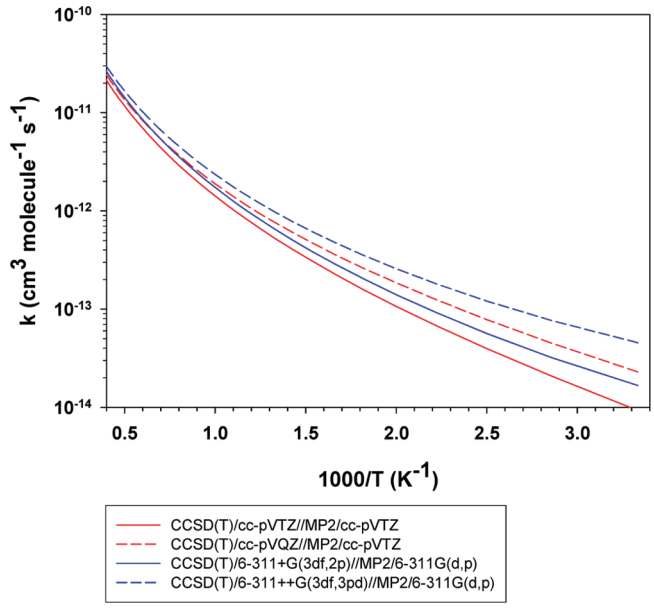

Figure 12. Temperature dependence of the rate constant of the reaction IO + HI → HOI + I ($^2P_{3/2}$) (R_{-4}).

spectrometric − discharge flow method at 320 K and 1 Torr. The total rate constant was determined from the kinetics of HOI consumption in an excess of OH radicals. The derived value was reported to be equal to $(5.0 \pm 1.2) \times 10^{-12}$ cm^3 molecule^{-1} s^{-1}. This value is shown in Figure 7 for comparison purposes. The values of the rate constants calculated at 320 K at the CCSD(T)/cc-pVTZ//MP2/cc-pVTZ, CCSD(T)/cc-pVQZ//MP2/cc-pVTZ, CCSD(T)/6-311+G(3df,2p)//MP2/6-311G(d,p), and CCSD(T)/6-311++G(3df,3pd)//MP2/6-311G(d,p) levels of theory are 7.19×10^{-13}, 6.32×10^{-13}, 1.64×10^{-13}, and 4.26×10^{-13} cm^3 molecule^{-1} s^{-1}, respectively. As expected, it can be noticed that our calculated rate constants for the H-abstraction channel are lower than the observed global rate constants. The differences between the computed rate constants and the global rate constants are less than 1 order of magnitude for almost all levels of theory.

Arrhenius Parameters. The modified three-parameter Arrhenius expressions, $k(T) = A \times T^n \exp(-E_a/RT)$, fitted to the rate constants computed at the four levels of theory over the temperature range 300−2500 K are reported in Table 8. Following our previous methodological work on the reaction of iodine atoms with H_2, H_2O, HI, and OH,[10] we are confident in our

Table 8. Summary of the Arrhenius Parameters Calculated over the Temperature Range of 300−2500 K for the Studied Reactions

reaction	SPC level of theory	A^a	n	$E_a{}^b$
HOI + H → IO + H_2 (R_1)	CCSD(T)/cc-pVTZ//MP2/cc-pVTZ	1.6×10^{-23}	3.64	18.0
	CCSD(T)/cc-pVQZ//MP2/cc-pVTZ	1.4×10^{-23}	3.66	18.3
	CCSD(T)/6-311+G(3df,2p)//MP2/6-311G(d,p)	8.8×10^{-24}	3.69	20.6
	CCSD(T)/6-311++G(3df,3pd)//MP2/6-311G(d,p)	1.7×10^{-23}	3.61	19.8
IO + H_2 → HOI + H (R_{-1})	CCSD(T)/cc-pVTZ//MP2/cc-pVTZ	1.2×10^{-24}	3.98	44.4
	CCSD(T)/cc-pVQZ//MP2/cc-pVTZ	1.1×10^{-24}	4.00	43.8
	CCSD(T)/6-311+G(3df,2p)//MP2/6-311G(d,p)	5.9×10^{-25}	4.06	48.2
	CCSD(T)/6-311++G(3df,3pd)//MP2/6-311G(d,p)	1.1×10^{-24}	3.98	43.4
HOI + OH → IO + H_2O (R_2)	CCSD(T)/cc-pVTZ//MP2/cc-pVTZ	3.6×10^{-27}	4.41	−19.9
	CCSD(T)/cc-pVQZ//MP2/cc-pVTZ	7.2×10^{-27}	4.33	−19.0
	CCSD(T)/6-311+G(3df,2p)//MP2/6-311G(d,p)	1.1×10^{-27}	4.49	−18.0
	CCSD(T)/6-311++G(3df,3pd)//MP2/6-311G(d,p)	5.1×10^{-27}	4.30	−19.2
IO + H_2O → HOI + OH (R_{-2})	CCSD(T)/cc-pVTZ//MP2/cc-pVTZ	1.6×10^{-27}	4.63	59.3
	CCSD(T)/cc-pVQZ//MP2/cc-pVTZ	3.2×10^{-27}	4.54	65.4
	CCSD(T)/6-311+G(3df,2p)//MP2/6-311G(d,p)	4.1×10^{-28}	4.74	67.0
	CCSD(T)/6-311++G(3df,3pd)//MP2/6-311G(d,p)	1.9×10^{-27}	4.56	64.3
HOI + O (^{3}P) → IO + OH (R_3)	CCSD(T)/cc-pVTZ//MP2/cc-pVTZ	3.4×10^{-28}	4.90	4.4
	CCSD(T)/cc-pVQZ//MP2/cc-pVTZ	2.8×10^{-27}	4.65	2.5
	CCSD(T)/6-311+G(3df,2p)//MP2/6-311G(d,p)	3.8×10^{-28}	4.88	−2.9
	CCSD(T)/6-311++G(3df,3pd)//MP2/6-311G(d,p)	2.3×10^{-27}	4.66	−4.9
IO + OH → HOI + O (^{3}P) (R_{-3})	CCSD(T)/cc-pVTZ//MP2/cc-pVTZ	1.2×10^{-29}	5.18	11.9
	CCSD(T)/cc-pVQZ//MP2/cc-pVTZ	9.5×10^{-29}	4.93	17.0
	CCSD(T)/6-311+G(3df,2p)//MP2/6-311G(d,p)	1.2×10^{-29}	5.19	12.3
	CCSD(T)/6-311++G(3df,3pd)//MP2/6-311G(d,p)	7.1×10^{-29}	4.98	10.0
HOI + I ($^2P_{3/2}$) → IO + HI (R_4)	CCSD(T)/cc-pVTZ//MP2/cc-pVTZ	3.6×10^{-18}	2.29	119.4
	CCSD(T)/cc-pVQZ//MP2/cc-pVTZ	3.8×10^{-18}	2.29	110.6
	CCSD(T)/6-311+G(3df,2p)//MP2/6-311G(d,p)	9.8×10^{-19}	2.46	117.0
	CCSD(T)/6-311++G(3df,3pd)//MP2/6-311G(d,p)	9.9×10^{-19}	2.46	111.7
IO + HI → HOI + I ($^2P_{3/2}$) (R_{-4})	CCSD(T)/cc-pVTZ//MP2/cc-pVTZ	3.0×10^{-19}	2.36	7.8
	CCSD(T)/cc-pVQZ//MP2/cc-pVTZ	3.0×10^{-19}	2.36	5.6
	CCSD(T)/6-311+G(3df,2p)//MP2/6-311G(d,p)	7.4×10^{-20}	2.56	5.8
	CCSD(T)/6-311++G(3df,3pd)//MP2/6-311G(d,p)	7.7×10^{-20}	2.55	3.3

[a] Units: cm^3 $molecule^{-1}$ s^{-1}. [b] Units: kJ mol^{-1}.

predicted Arrhenius parameters with the four different levels of theory for the eight studied elementary reactions.

CONCLUSION

Ab initio theoretical calculations combined with canonical TST were performed on the reactions of HOI with H, OH, O (^{3}P), and iodine atoms ($^2P_{3/2}$). The geometry parameters for reactants, products, molecular complexes, and TSs were fully optimized with the MP2 method combined with the cc-pVTZ and 6-311G(d,p) basis sets. The rate constants computed over the temperature range 300−2500 K have been fitted with a modified three-parameter Arrhenius expression using the CCSD(T)/cc-pVnZ//MP2/cc-pVTZ (n = T and Q), CCSD(T)/6-311+G(3df,2p)//MP2/6-311G(d,p), and CCSD(T)/6-311++G(3df,3pd)//MP2/6-311G(d,p) levels of theory. In light of the observed trends in our previous study,[10] the use of the CCSD(T)/cc-pVQZ//MP2/cc-pVTZ and CCSD(T)/6-311++G(3df,3pd) levels of theory is recommended. These Arrhenius parameters are therefore recommended for use in the development of a gaseous kinetic network, which could be implemented in severe accident simulation software such as ASTEC[7,8] for instance.

ASSOCIATED CONTENT

Supporting Information. Additional tables as described in the text. This material is available free of charge via the Internet at http://pubs.acs.org.

AUTHOR INFORMATION

Corresponding Author

*Phone: (33)3-20436977; e-mail: sebastien.canneaux@univ-lille1.fr.

ACKNOWLEDGMENT

We thank the Grand Equipement National de Calcul Intensif (GENCI) - Institut du Développement et des Ressources en Informatique Scientifique (IDRIS), the ROMEO2 Computational Center of the University of Reims Champagne-Ardenne,

the Centre de Ressources Informatiques de Haute Normandie (CRIHAN), and the Centre de Ressources Informatiques (CRI) of the University of Lille 1 for providing computing time for part of the theoretical calculations. We thank the Nord Pas de Calais Region, the European funds for Regional Economic Development and the Air Quality Program of the Institut de Recherche en ENvironnment Industriel, and EDF for their financial support. The authors thank also Hanae Amalik and Damien Duquenne.

REFERENCES

(1) Wren, J. C.; Ball, J. M.; Glowa, G. A. *Nucl. Technol.* **2000**, *129*, 297–325.

(2) Dickinson, S.; Andreo, F.; Karkela, T.; Ball, J.; Bosland, L.; Cantrel, L.; Funke, F.; Girault, N.; Holm, J.; Guilbert, S.; Herranz, L. E.; Housiadas, C.; Ducros, G.; Mun, C.; Sabroux, J.-C.; Weber, G. *Prog. Nucl. Energy* **2010**, *52*, 128–135.

(3) Institut de Radioprotection et de Sûreté Nucléaire: http://www.irsn.fr.

(4) Séropian, C.; Cantrel, L.; Cousin, F. *CSARP Meeting*, Bethesda Maryland, USA, September 14−16, 2010.

(5) Ohnet, M. N.; Jacquemain, D.; Alpy, N.; Giordano, P.; Cantrel, L.; Kissane, M.; Clément, B.; Beyly, D.; Bouriot, P. *CHIP Programme Strategy*, Internal Technical report 2004, DPAM/DIR/2004-0347 rev. A.

(6) Clément, B.; Zeyen, R. *International Conference, Nuclear Energy for New Europe*; Bled, Slovenia, September 5−8, 2005.

(7) Van Dorsselaere, J. P.; Seropian, C.; Chatelard, P.; Jacq, F.; Fleurot, J.; Giordano, P.; Reinke, N.; Schwinges, B.; Allelein, H. J.; Luther, W. *Nucl. Technol.* **2009**, *165*, 293–307.

(8) Cousin, F.; Dieschbourg, K.; Jacq, F. *Nucl. Eng. Des.* **2008**, *238*, 2430–2438.

(9) Mečiarová, K.; Cantrel, L.; Černušák, I. *Collect. Czech. Chem. Commun.* **2008**, *73*, 1340–1356.

(10) Canneaux, S.; Xerri, B.; Louis, F.; Cantrel, L. *J. Phys. Chem. A* **2010**, *114*, 9270–9288.

(11) Lin, C. C. *J. Inorg. Nucl. Chem.* **1981**, *43*, 3229–3238.

(12) Voilleque, P. G.; Keller, J. H. *Health Phys.* **1981**, *40*, 91–94.

(13) Begović, N.; Marković, Z.; Anić, S.; Kolar-Anić, L. *J. Phys. Chem. A* **2004**, *108*, 651–657.

(14) Noguchi, H.; Murata, M. *J. Environ. Radioact.* **1988**, *7*, 65–74.

(15) Cline, J. E.; Voilleque, P. G.; Pelletier, C. A.; Thomas, C. D. *16th DOE Nuclear Air Cleaning Conference*, San Diego, CA, USA, September 14−16, 1981.

(16) Clément, B.; Hanniet-Girault, N.; Repetto, G.; Jacquemain, D.; Jones, A. V.; Kissane, M. P.; von der Hardt, P. *Nucl. Eng. Des.* **2003**, *226*, 5–82.

(17) Cantrel, L.; Krausmann, E. *Nucl. Technol.* **2003**, *144*, 1–15.

(18) Marshall, P. *Adv. Quantum Chem.* **2008**, *55*, 159–175.

(19) Berry, R. J.; Yuan, J.; Misra, A.; Marshall, P. *J. Phys. Chem. A* **1998**, *102*, 5182–5188.

(20) Hassanzadeh, P.; Irikura, K. K. *J. Phys. Chem. A* **1997**, *101*, 1580–1587.

(21) Frisch, M. J.; Trucks, G. W.; Schlegel, H. B.; Scuseria, G. E.; Robb, M. A.; Cheeseman, J. R.; Montgomery, Jr., J. A.; Vreven, T.; Kudin, K. N.; Burant, J. C.; Millam, J. M.; Iyengar, S. S.; Tomasi, J.; Barone, V.; Mennucci, B.; Cossi, M.; Scalmani, G.; Rega, N.; Petersson, G. A.; Nakatsuji, H.; Hada, M.; Ehara, M.; Toyota, K.; Fukuda, R.; Hasegawa, J.; Ishida, M.; Nakajima, T.; Honda, Y.; Kitao, O.; Nakai, H.; Klene, M.; Li, X.; Knox, J. E.; Hratchian, H. P.; Cross, J. B.; Bakken, V.; Adamo, C.; Jaramillo, J.; Gomperts, R.; Stratmann, R. E.; Yazyev, O.; Austin, A. J.; Cammi, R.; Pomelli, C.; Ochterski, J. W.; Ayala, P. Y.; Morokuma, K.; Voth, G. A.; Salvador, P.; Dannenberg, J. J.; Zakrzewski, V. G.; Dapprich, S.; Daniels, A. D.; Strain, M. C.; Farkas, O.; Malick, D. K.; Rabuck, A. D.; Raghavachari, K.; Foresman, J. B.; Ortiz, J. V.; Cui, Q.; Baboul, A. G.; Clifford, S.; Cioslowski, J.; Stefanov, B. B.; Liu, G.; Liashenko, A.; Piskorz, P.; Komaromi, I.; Martin, R. L.; Fox, D. J.; Keith, T.; Al-Laham, M. A.; Peng, C. Y.; Nanayakkara, A.; Challacombe, M.; Gill, P. M. W.; Johnson, B.; Chen, W.; Wong, M. W.; Gonzalez, C.; and Pople, J. A. *Gaussian 03*, revision D.01, Gaussian, Inc.: Wallingford, CT, 2004.

(22) Møller, C.; Plesset, M. S. *Phys. Rev.* **1934**, *46*, 618–622.

(23) (a) Dunning, T. H., Jr. *J. Chem. Phys.* **1989**, *90*, 1007–1023. (b) Kendall, R. A.; Dunning, T. H., Jr.; Harrison, R. J. *J. Chem. Phys.* **1992**, *96*, 6796–6806. (c) Woon, D. E.; Dunning, T. H., Jr. *J. Chem. Phys.* **1993**, *98*, 1358–1371. (d) Peterson, K. A.; Woon, D. E.; Dunning, T. H., Jr. *J. Chem. Phys.* **1994**, *100*, 7410–7415. (e) Wilson, A. K.; van Mourik, T.; Dunning, T. H., Jr. *J. Mol. Struct. (THEOCHEM)* **1996**, *388*, 339–349.

(24) Descriptions of the Pople-type basis sets can be found in the following:Foresman, J. B.; Frisch, A. E. *Exploring Chemistry with Electronic Structure Methods*, 2nd ed.; Gaussian, Inc.: Pittsburgh, PA, 1996.

(25) Peterson, K. A.; Shepler, B. C.; Figgen, D.; Stoll, H. *J. Phys. Chem. A* **2006**, *110*, 13877–13883.

(26) McLean, A. D.; Chandler, G. S. *J. Chem. Phys.* **1980**, *72*, 5639–5648.

(27) Glukhovtsev, M. N.; Pross, A.; McGrath, M. P.; Radom, L. *J. Chem. Phys.* **1995**, *103*, 1878–1885.

(28) (a) Gonzalez, C.; Schlegel, H. B. *J. Chem. Phys.* **1989**, *90*, 2154–2161. (b) Gonzalez, C.; Schlegel, H. B. *J. Phys. Chem.* **1990**, *94*, 5523–5527.

(29) (a) Cizek, J. *Adv. Chem. Phys.* **1969**, *14*, 35–89. (b) Purvis, G. D., III; Bartlett, R. J. *J. Chem. Phys.* **1982**, *76*, 1910–1918. (c) Scuseria, G. E.; Janssen, C. L.; Schaefer, H. F., III. *J. Chem. Phys.* **1988**, *89*, 7382–7387. (d) Scuseria, G. E.; Schaefer, H. F., III. *J. Chem. Phys.* **1989**, *90*, 3700–3703. (e) Pople, J. A.; Head-Gordon, M.; Raghavachari, K. *J. Chem. Phys.* **1987**, *87*, 5968–5975.

(30) Lee, S.-H.; Liu, K. *J. Chem. Phys.* **1999**, *111*, 6253–6259.

(31) Jasper, A. W.; Klippenstein, S. J.; Harding, L. B. *J. Phys. Chem. A* **2010**, *114*, 5759–5768.

(32) Moore, C. E. *Atomic Energy Levels*; U.S. GPO: Washington, DC, 1971; Vols. II and III, NSRDS-NBS 35.

(33) Stevens, J. E.; Cui, Q.; Morokuma, K. *J. Chem. Phys.* **1998**, *108*, 1544–1551.

(34) Gilles, M K.; Polak, M. L.; Lineberger, W. C. *J. Phys. Chem.* **1991**, *95*, 4723–4724.

(35) NIST Computational Chemistry Comparison and Benchmark Database; Johnson, R. D., III, Ed.; NIST Standard Reference Database Number 101 Release 15a, April 2010. http://cccbdb.nist.gov/

(36) Feller, D.; Peterson, K. A.; de Jong, W. A.; Dixon, D. A. *J. Chem. Phys.* **2003**, *118*, 3510–3522.

(37) Singleton, D. L.; Cvetanovic, R. J. *J. Am. Chem. Soc.* **1976**, *98*, 6812–6819.

(38) (a) Eyring, H. *J. Chem. Phys.* **1935**, *3*, 107–115.(b) Johnston, H. S. *Gas Phase Reaction Rate Theory*; The Roland Press Co.: New York, 1966. (c) Laidler, K. J. *Theories of Chemical Reaction Rates*; McGraw-Hill: New York, 1969. (d) Weston, R. E.; Schwartz, H. A.*Chemical Kinetics*; Prentice-Hall: New York, 1972. (e) Rapp, D. *Statistical Mechanics*; Holt, Reinhard, and Winston: New York, 1972. (f) Nikitin, E. E. *Theory of Elementary Atomic and Molecular Processes in Gases*; Claredon Press: Oxford, 1974. (g) Smith, I. W. M. *Kinetics and Dynamics of Elementary Gas Reactions*; Butterworths: London, 1980. (h) Steinfeld, J. I.; Francisco, J. S.; Hase, W. L. *Chemical Kinetics and Dynamics*; Prentice-Hall: Englewood Cliffs, NJ, 1989.

(39) Eckart, C. *Phys. Rev.* **1930**, *35*, 1303–1309.

(40) Brown, R. L. *J. Res. Natl. Bur. Stand. (U.S.)* **1981**, *86*, 357–359.

(41) Henon, E.; Bohr, F.; Canneaux, S.; Postat, B.; Auge, F.; Bouillard, E.; Domureau, V. *KISTHEP 1.0*; University of Reims Champagne-Ardenne: France, 2003.

(42) Rayez, M. T.; Rayez, J. C.; Sawerysyn, J. P. *J. Phys. Chem.* **1994**, *98*, 11342–11352.

(43) Hammond, G. S. *J. Am. Chem. Soc.* **1955**, *77*, 334–338.

(44) Chase Jr., M. W. NIST-JANAF Thermochemical Tables, *J. Phys. Chem. Ref. Data* **1998**, Monograph 9.

(45) Dooley, K. S.; Geidosch, J. N.; North, S. W. *Chem. Phys. Lett.* **2008**, *457*, 303–306.

(46) Riffault, V.; Bedjanian, Y.; Poulet, G. *J. Photochem. Photobiol. A: Chem.* **2005**, *176*, 155–161.